

pubs.acs.org/JCTC Article

Toward Linear Scaling Auxiliary-Field Quantum Monte Carlo with Local Natural Orbitals

Jo S. Kurian,* Hong-Zhou Ye, Ankit Mahajan, Timothy C. Berkelbach, and Sandeep Sharma



Cite This: J. Chem. Theory Comput. 2024, 20, 134-142



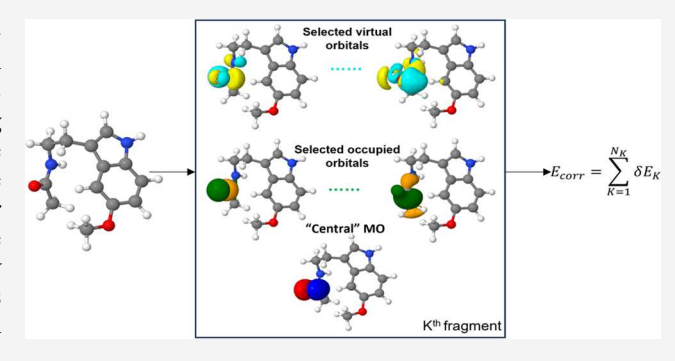
ACCESS I

III Metrics & More

Article Recommendations

SI Supporting Information

ABSTRACT: We develop a local correlation variant of auxiliary-field quantum Monte Carlo (AFQMC) based on local natural orbitals (LNO-AFQMC). In LNO-AFQMC, independent AFQMC calculations are performed for each localized occupied orbital using a truncated set of tailored orbitals. Because the size of this space does not grow with the system size for a target accuracy, the method has linear scaling. Applying LNO-AFQMC to molecular problems containing a few hundred to a thousand orbitals, we demonstrate convergence of total energies with significantly reduced costs. The savings are more significant for larger systems and larger basis sets. However, even for our smallest system studied, we find that LNO-AFQMC is cheaper than canonical



AFQMC, in contrast with many other reduced-scaling methods. Perhaps most significantly, we show that energy differences converge much more quickly than total energies, making the method ideal for applications in chemistry and material science. Our work paves the way for linear scaling AFQMC calculations of strongly correlated systems, which would have a transformative effect on ab initio quantum chemistry.

I. INTRODUCTION

The primary objective of the field of electronic structure theory is to develop cost-effective and accurate methods that can be applied to challenging problems with ease. Existing methods differ in the approximations they use to solve the Schrödinger equation, and often, the choice of method is limited by available computational resources. Although Kohn–Sham density functional theory (DFT) is the most widely used method, its accuracy is difficult to improve systematically. The coupled-cluster (CC) method with single, double, and perturbative triple excitations $[CCSD(T)]^2$ is widely regarded as the "gold standard" for its accuracy when applied to main group chemistry. However, the computational cost of canonical CCSD(T) scales with system size N as N^7 , which limits its practical application to small systems. Moreover, the CCSD-(T) fails catastrophically for strongly correlated systems.

The phaseless auxiliary-field quantum Monte Carlo $(AFQMC)^3$ method has gained popularity due to its comparatively low N^4 computational scaling (i.e., the same as mean-field theory) and impressive accuracy even for strongly correlated systems. $^{4-12}$ AFQMC is a descendent of the determinantal QMC method 13,14 and was extensively developed for electronic structure by Zhang and co-workers. Recent algorithmic developments aimed at reducing the cost of AFQMC include the use of low-rank Coulomb integrals, stochastic resolution of identity, and local trial states.

Even though AFQMC has a better formal scaling than the traditional correlated methods widely used in quantum

chemistry, it can still be computationally infeasible for larger systems due to a large prefactor. In this work, we overcome this limitation of AFQMC by the use of local correlation. The idea to use locality to reduce the cost of correlated calculations dates back to the early 70's,21 but local correlation was developed in its modern form by Pulay and Saebø in the 80's. 22-25 In this pioneering work, it was recognized that the electron correlation decays rapidly with the distance between the localized orbitals. This observation underpins so-called "direct" local correlation methods, in which a single calculation (almost exclusively perturbation theory or coupled-cluster theory) is performed on the basis of localized orbitals, permitting the discarding of small terms and resulting in a calculation with linear asymptotic scaling. Methods of this type have been extensively developed by many researchers.²⁶⁻³³ The revival of pair natural orbital-based local correlation methods^{34–36} by Neese, Valeev, and co-workers^{37–40} was a major advance of the past decade, and many related variants have since been developed.^{41–51} Within QMC, a linear scaling version of diffusion Monte Carlo was developed that used

Received: October 10, 2023
Revised: November 27, 2023
Accepted: November 28, 2023
Published: December 19, 2023





Wannier functions to calculate wave function overlaps with linear scaling. ⁵² This work was later extended to improve the scaling of local energy evaluation. ^{53–55}

A different approach to local correlation, often called fragment-based methods, was initiated by Förner and coworkers. S6,57 These methods partition the problem into subsystems, and separate calculations are performed on each subsystem. Many variants exist, including the incremental method, S8-65 divide and conquer, 66,67 divide-expand-consolidate, and cluster-in-molecule (CIM). A significant advantage of such fragment methods over direct methods is that they are easy to implement, can be easily modified for different electron correlation methods, and parallelize trivially. In this work, we combine AFQMC with the CIM approach, in particular, the local natural orbital (LNO)-based variant recently proposed by Kállay and co-workers. Importantly, we show that our fragment-based approach is cheaper than the canonical one, even for small system sizes.

The rest of the paper is organized as follows. In Section II, we present the basic theory of both LNO-based local correlation methods and canonical AFQMC with an emphasis on those aspects of AFQMC that will be modified to develop LNO-AFQMC. We end this section with an analysis of the computational scaling of LNO-AFQMC. In Section III, we compare the efficiency of LNO-AFQMC for calculating the absolute energies and relative energies compared to that of canonical AFQMC for molecules and reactions of different sizes using various basis sets. In Section IV, we conclude and suggest future research directions.

II. THEORY

In this work, we consider only closed-shell molecules described by a spin-restricted Hartree–Fock (HF) reference determinant $|\Phi_0\rangle$, with canonical HF orbitals ψ_p , orbital energies ϵ_p , and total energy $E_{\rm HF}$. We use i, j, and k for N_0 occupied orbitals, a, b, and c for N_v virtual orbitals, and p, q, r, and s for N unspecified molecular orbitals. In this basis, the electronic Hamiltonian is

$$H = \sum_{pq,\sigma}^{N} h_{pq} a_{p\sigma}^{\dagger} a_{q\sigma} + \frac{1}{2} \sum_{pqrs,\sigma\sigma'}^{N} V_{prqs} a_{p\sigma}^{\dagger} a_{q\sigma'}^{\dagger} a_{s\sigma'} a_{r\sigma}$$

$$\tag{1}$$

with $V_{pqrs} = (pq|rs)$ in (11|22) notation.

II.I. LNO Coupled-Cluster Theory. For completeness, we describe the basics of the LNO–CCSD method. 73–77 In this approach, the correlation energy is obtained by left projection onto the HF determinant,

$$E_{c} = \langle \Phi_{0} | \overline{H} - E_{HF} | \Phi_{0} \rangle = \sum_{ijab} T_{iajb} \left(2V_{iajb} - V_{ibja} \right) = \sum_{I} E_{I}$$
(2)

where \overline{H} is the similarity-transformed Hamiltonian, $T_{iajb} = t_{iajb} + t_{ia}t_{jb}$ and t_{ja} , t_{iajb} are the CC single and double amplitudes, respectively. In the final equality of eq 2, we have recognized that the energy expression is invariant to unitary rotations of occupied and virtual orbitals and associated an energy contribution to each rotated occupied orbital

$$\phi_{I} = \sum_{i} U_{iI} \psi_{i} \tag{3}$$

In LNO methods, the unitary transformation of occupied orbitals (eq 3) is chosen to spatially localize the orbitals. For each ϕ_{li} one constructs a local active space \mathcal{P}_{li} by augmenting

 ϕ_I with selected LNOs (both occupied and virtual) from second-order Møller–Plesset perturbation theory (MP2). Specifically, one computes the occupied–occupied and the virtual–virtual blocks of the MP2 density matrix

$$D_{ij}^{I} = \sum_{ab} t_{iaIb}^{(1)} \left[2t_{jaIb}^{(1)} - t_{Iajb}^{(1)} \right]$$
 (4)

$$D_{ab}^{I} = \sum_{jc} t_{Iajc}^{(1)} \left[2t_{Ibjc}^{(1)} - t_{jbIc}^{(1)} \right]$$
(5)

where

$$t_{Iajb}^{(1)} = \frac{(Ialjb)}{\tilde{\epsilon}_I + \epsilon_j - \epsilon_a - \epsilon_b} \tag{6}$$

is an approximate MP2 amplitude with $\tilde{\epsilon}_I = \langle \phi_I | f | \phi_I \rangle$ and f is the Fock operator. Diagonalizing the virtual–virtual block,

$$D_{ab}^{I} = \sum_{c} \xi_{c}^{I} X_{ac}^{I} X_{bc}^{I} \tag{7}$$

gives the virtual LNOs associated with ϕ_D i.e., $\phi_b = \sum_c X_{cb}^I \psi_c$ For the occupied LNOs, we follow ref 73 and diagonalize

$$\tilde{D}_{ij}^{I} = \sum_{kl} Q_{ik}^{I} D_{kl}^{I} Q_{lj}^{I} = \sum_{k}^{N_0 - 1} \xi_k^{I} X_{ik}^{I} X_{jk}^{I}$$
(8)

where $Q_{ij}^I = \delta_{ij} - U_{iI}U_{jI}$ projects out ϕ_I from D_{ij}^I to prevent it from mixing with other occupied orbitals, giving the occupied LNOs $\phi_j = \sum_k X_{kj}^I \psi_k$. The eigenvalues ξ_{p}^I , which are between 2 and 0, quantify the importance of a given LNO to the electron correlation of the localized orbital ϕ_I . In practice, we construct the local active space \mathcal{P}_I by keeping those LNOs satisfying

$$\xi_i \ge \epsilon_o, \ \xi_a \ge \epsilon_v \tag{9}$$

for some user-selected thresholds $\epsilon_{\rm o}$ and $\epsilon_{\rm v}$, producing $n=n_0+n_{\rm v}$ orbitals. Typically, n is much less than N and does not increase with the system size for a targeted level of accuracy. A local Hamiltonian is then constructed by projecting H into \mathcal{P}_I

$$H_{I} = \sum_{pq \in \mathcal{P}_{l}, \sigma}^{n} f_{pq}^{I} a_{p\sigma}^{\dagger} a_{q\sigma} + \frac{1}{2} \sum_{pqrs \in \mathcal{P}_{l}, \sigma\sigma'}^{n} V_{prqs} a_{p\sigma}^{\dagger} a_{q\sigma'}^{\dagger} a_{s\sigma'} a_{r\sigma'}$$

$$\tag{10}$$

where

$$f_{pq}^{I} = h_{pq} + \sum_{j \notin \mathcal{P}_{I}}^{N_{0} - n_{0}} (2V_{pqjj} - V_{pjjq})$$
(11)

which includes a frozen core contribution. Solving the CCSD amplitude equations with H_I gives the local CCSD amplitudes T_{Iajb} in \mathcal{P}_I and the associated orbital contribution to the correlation energy

$$E_I = \sum_{jab \in \mathcal{P}_I} T_{Iajb} (2V_{Iajb} - V_{jaIb}) \tag{12}$$

LNO-CCSD(T) calculations are performed in a similar way, as described in more detail in refs 74 and 75. We note that other fragment-based local correlation methods follow essentially the same idea but differ only in the definition of the local fragments I and the method for constructing the associated active space of orbitals \mathcal{P}_I .

II.II. LNO-AFQMC. Adapting the LNO approach for use with AFQMC merely requires an energy expression analogous

to that in eq 2. This is straightforward given that the AFQMC energy is also obtained by left projection onto a trial state, which throughout this work we choose to be the HF determinant $|\Phi_0\rangle$. In AFQMC, the ground state is represented as a statistical average of walkers, each a single Slater determinant $|\Phi_w\rangle$, with weight W_w

$$|\Psi\rangle = \frac{\sum_{w} W_{w} |\Phi_{w}\rangle}{\sum_{w} W_{w}} \tag{13}$$

a review of the AFQMC method with further technical details can be found in ref 3. The correlation energy is

$$E_{\rm c} = \frac{\sum_{\scriptscriptstyle w} W_{\scriptscriptstyle w} E_{\rm c}^{\scriptscriptstyle w}}{\sum_{\scriptscriptstyle w} W_{\scriptscriptstyle w}} \tag{14a}$$

$$E_{\rm c}^{\scriptscriptstyle W} = \frac{\langle \Phi_0 | H - E_{\rm HF} | \Phi_{\scriptscriptstyle W} \rangle}{\langle \Phi_0 | \Phi_{\scriptscriptstyle W} \rangle} \tag{14b}$$

By expanding the walker determinant in the basis of excitations with respect to the HF trial state, the correlation energy of a given walker is easily evaluated to be

$$E_c^w = \sum_{ijab} G_{ia}^w G_{jb}^w (2V_{iajb} - V_{ibja}) = \sum_I E_I^w$$
(15)

where $G_{ia}^{w} = \langle \Phi_0 | a_i^{\dagger} a_a | \Phi_w \rangle / \langle \Phi_0 | \Phi_w \rangle$ is the generalized one-particle reduced density matrix. Equation 15 clearly has the same form as the CCSD in expression 2. Thus, in LNO-AFQMC, we form localized occupied orbitals and associated local active spaces \mathcal{P}_I just as in LNO-CCSD; we then perform independent AFQMC calculations in each local active space \mathcal{P}_I and calculate the contribution E_I to the correlation energy as an average over walkers,

$$E_I = \frac{\sum_{w} W_w E_I^w}{\sum_{w} W_w} \tag{16a}$$

$$E_{I}^{w} = \sum_{jab \in \mathcal{P}_{I}} G_{Ia}^{w} G_{jb}^{w} (2V_{Iajb} - V_{jaIb})$$
(16b)

This general form is amenable to almost any flavor of fragment-based local correlation, although here we focus on the LNO framework. In this work, we perform AFQMC calculations with the phaseless approximation and force bias (hybrid) importance sampling. We note that if a multi-determinant trial wave function is used, then expressing the correlation energy as a sum of contributions becomes more complicated because there is not a unique set of occupied orbitals. This extension will require a different partitioning of the correlation energy that ensures that scaling with the number of configurations is manageable for each independent calculation. These aspects will be explored in future investigations.

In practice, the missing correlation outside of \mathcal{P}_I can be included approximately by a composite correction with a lower level of theory, such as MP2. To any LNO calculation (CC or AFQMC), we add the correction

$$\Delta E^{(2)} = E_{\rm c}^{(2)} - E_{\rm c,LNO}^{(2)} \tag{17}$$

where $E_{\rm c}^{(2)}$ and $E_{\rm c,LNO}^{(2)}$ are the MP2 correlation energies in the full orbital space and in the truncated LNO space, respectively.

Summarizing the steps and cost of an LNO calculation, there are three parts.

- Full-system MP2, which is required by both the LNO construction [eqs 4-8] and the MP2 composite correction [eq 17] and scales as O(N⁵).
- 2. N_0 independent integral transformations, which are required by the local Hamiltonian construction [eq 10] and scale as $O(N^4n)$ each, but embarrassingly parallel in N_0 .
- 3. Independent correlated calculations of all local Hamiltonians, which scale as N_0 times the cost of a calculation at the desired level of theory in the local active space, i.e., n^4 for AFQMC, n^6 for CCSD, and n^7 for CCSD(T).

For moderately sized systems, the high-level correlated calculation in step (3) dominates the computational cost, which leads to an overall cost that scales linearly with the system size. This will be the case for all of the systems we use to benchmark our method in this work. As the system size increases, the first two steps whose cost scales superlinearly with the system size N eventually become the computational bottleneck. Although not explored in this work, many numerical techniques such as local domain-based approximations 74 and Laplace transform methods 75 have been exploited to make these steps linear scaling as well. Such advances can be straightforwardly used with the LNO-AFQMC approach described here.

II.III. Computational Scaling of AFQMC and LNO-AFQMC. In AFQMC, energies are obtained by averaging over a trajectory that samples the wave function. With force bias (hybrid) importance sampling, the cost of each propagation step scales as N^3 . Local energy evaluation scales as N^4 but is performed less frequently; for moderately sized systems, including those studied here, the total cost is dominated by propagation and thus scales effectively as N^3 . However, for the following scaling analysis, we will assume the worst-case scenario where local energy evaluation dominates, although we note that its scaling can be reduced to N^3 using integral compression 16,17,19 or localized orbitals. 18

The above scalings are for a trajectory with a fixed number of iterations, $N_{\rm t}$ but how does $N_{\rm t}$ scale with system size N? Assuming the variance of the total energy is proportional to system size, the stochastic error after $N_{\rm t}$ iterations is $\sqrt{\sigma^2/N_{\rm t}} \propto \sqrt{N/N_{\rm t}}$. Therefore, to achieve a fixed absolute error requires $N_{\rm t} \propto N$ but to achieve a fixed relative error (i.e., error per electron) requires $N_{\rm t} \propto 1/N$. Thus, for a calculation dominated by N^4 -scaling energy evaluation, the final cost of AFQMC scales as N^5 for fixed absolute error and as N^3 for fixed relative error.

In LNO-AFQMC, the computational scaling of a single propagation step (including local energy evaluation) is effectively reduced from N^4 to Nn^4 , where n is independent of the system size because each fragment is treated independently. This reduction by a factor of N^3 implies that the cost of LNO-AFQMC scales as N^2 for fixed absolute error and is independent of N for the fixed relative error (to be compared to N^5 and N^3 , respectively, for the canonical algorithm).

Separately, one needs to consider the biases inherent in AFQMC results due to Trotter error and truncation of the Cholesky decomposition of the two-electron integrals. In both cases, we expect the errors to increase with the size of the system for a fixed time step and Cholesky threshold. Thus, to obtain a constant error with increasing system size, one has to run calculations with smaller time steps and a Cholesky

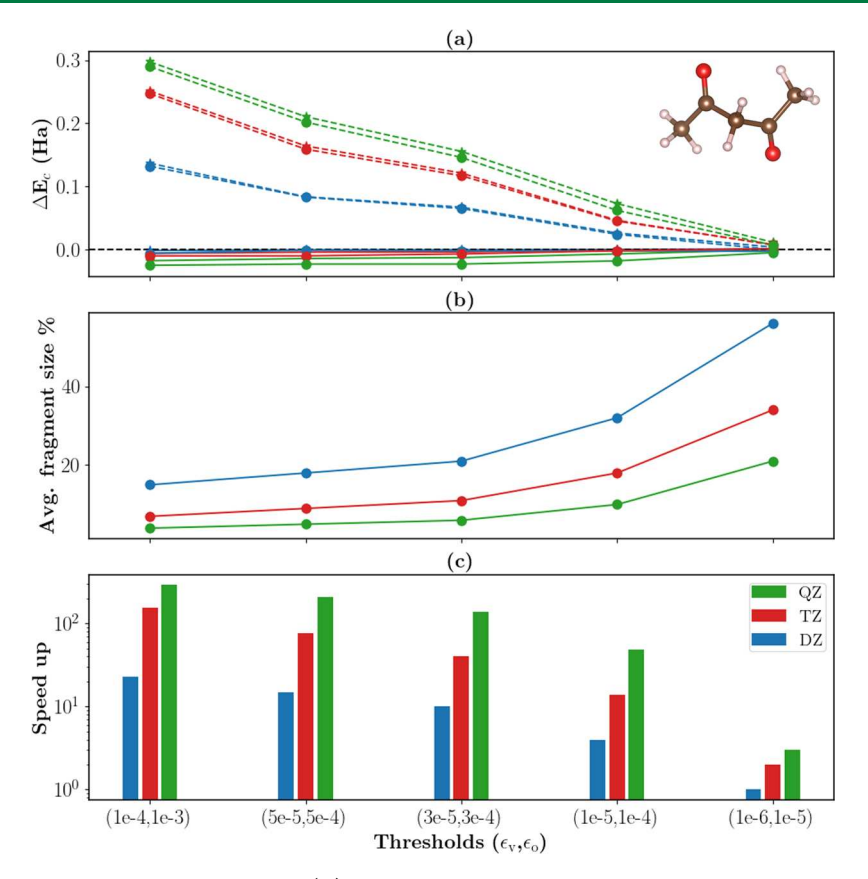


Figure 1. Performance of LNO-AFQMC and LNO-CCSD(T) for the total correlation energy of the acetylacetone molecule (shown in the inset). (a) Convergence of the correlation energy of LNO-AFQMC (circles) and LNO-CCSD(T) (star), with (solid lines) and without (dashed lines) MP2 corrections in the DZ (blue), TZ (red), and QZ (green) basis sets. (b) The average number of orbitals in each LNO fragment as a percentage of the total number of molecular orbitals. (c) Speed-up of LNO-AFQMC compared to canonical AFQMC, where the timing of LNO-AFQMC is reported as the sum of times for all fragments.

threshold. In LNO-AFQMC, these shortcomings are mitigated because each individual calculation contains a small number of electrons. Empirically, we find that in LNO-AFQMC calculations, we can use a Cholesky threshold that is an order of magnitude larger than in canonical AFQMC calculations without seeing a noticeable error in the final results (see Section III). Similarly, we find that in large AFQMC calculations, we need to use smaller Trotter time steps to avoid large biases.

III. RESULTS

In this section, we present the results of LNO-AFQMC calculations for total energies and isomerization reaction energies. Tight convergence of total energies is naturally more difficult to achieve than that of energy differences. All HF, MP2, and CC calculations were performed using PySCF, and all AFQMC calculations were performed using Dice that a Trotter time step of 0.005 au, unless specified otherwise. The geometries used for the total energy calculations are provided in the Supporting Information. For all calculations, Dunning correlation-consistent basis sets [cc-pVXZ (where X = D,T,Q) or aug-cc-pVDZ] $^{82-84}$ were used. The core electrons were kept frozen in all of the calculations.

Occupied orbitals were localized using the Pipek–Mezey method. Following previous work, a ratio of $\epsilon_{\rm o}/\epsilon_{\rm v}=10$ was fixed to reduce the number of variables, and we generally test the range from $\epsilon_{\rm v}=10^{-4}$ (loosest) to $\epsilon_{\rm v}=10^{-6}$ (tightest). In the LNO-AFQMC fragments, Cholesky decomposition was

performed with a threshold error of 1×10^{-4} , while for the reference AFQMC calculations, a more stringent threshold error of 1×10^{-5} was employed. All LNO-AFQMC calculations were converged to 1 mHa stochastic error, which requires converging the correlation energy contribution from each fragment to a stochastic error that is smaller by a factor of $\sqrt{N_0}$, where N_0 is the number of fragments (equal to the number of occupied orbitals). For canonical AFQMC calculations, a stochastic error of 1 mHa can be achieved for small molecules but not for large basis sets and large molecules without significant computer resources.

III.I. Total Energies. Total energy calculations were performed on acetylacetone, which is small enough (40 valence electrons) to allow canonical CCSD(T) and AFQMC calculations in the DZ (131 orbitals), TZ (315 orbitals), and QZ (618 orbitals) basis sets for benchmarking purposes. In Figure 1(a), we show the convergence of the correlation energy with the LNO threshold using different basis sets. Without the MP2 correction, the correlation energy error is large but progressively converges with tighter thresholds. The convergence is significantly accelerated with the MP2 correction. Specifically, in the DZ basis (with the MP2 correction), the correlation energy error is 6 mHa with loose thresholds and 3 mHa with tight thresholds, the latter of which is comparable to the stochastic error of calculation. Similarly, in the TZ and QZ basis sets, the error decreases from 10 to 1 mHa and from 25 to 3 mHa with increasingly tight thresholds. We note that all of these errors amount to less than

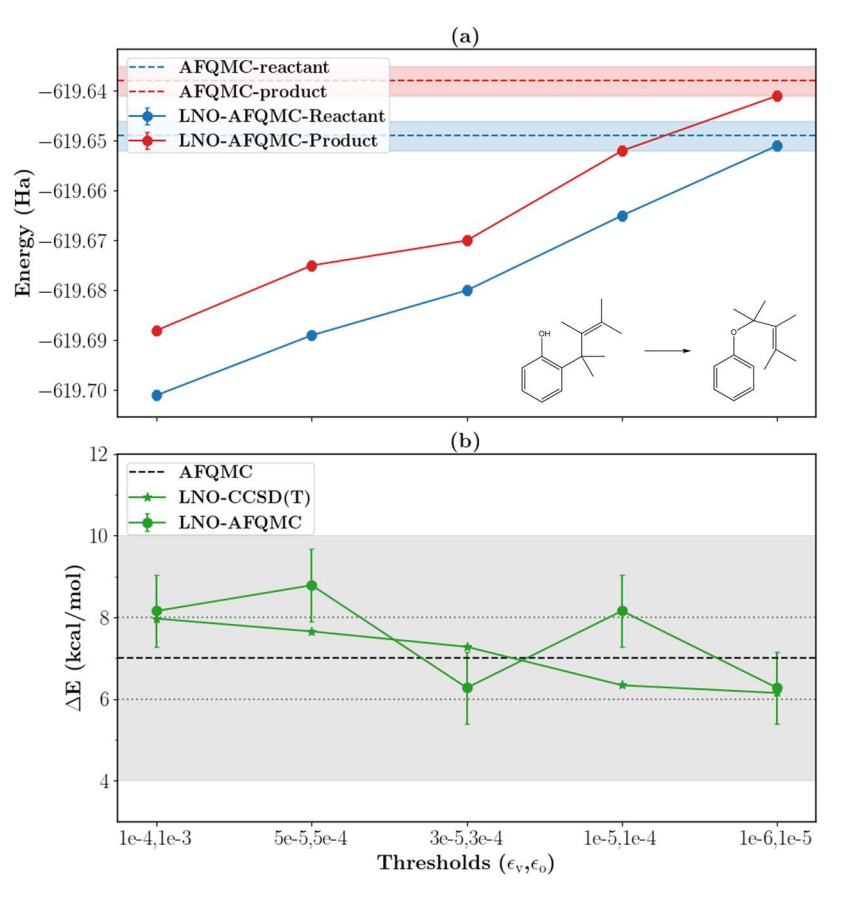


Figure 2. Performance of LNO-AFQMC (with MP2 corrections) for the isomerization energy of reaction 10 from the ISOL database [shown in (a)] with the cc-pVTZ basis set. Convergence of the total energy of the reactant and the product (a) and their energy difference (b) as a function of threshold. The red, blue, and gray shaded regions indicate the stochastic error of the canonical AFQMC calculations, and the dotted lines indicate ±1 kcal/mol around the average canonical AFQMC isomerization energy.

2% of the total correlation energy. This convergence behavior is almost identical with that from LNO-CCSD(T), results of which are also shown in Figure 1(a), confirming the straightforward transferability of the LNO methodology. Therefore, the general guidelines used for LNO-CCSD(T) in choosing thresholds can be readily extended to LNO-AFQMC.

As discussed above, the key advantage of the LNO methodology is the reduction in the number of orbitals that must be correlated within each fragment. In Figure 1(b), we show the average size (total number of orbitals) of the LNO fragments of acetylacetone with the DZ, TZ, and QZ basis sets. Even with the tightest threshold, the average number of fragment orbitals is 56, 34, and 21% of the total number of orbitals in DZ, TZ, and QZ basis sets, respectively, showing that the method is particularly advantageous for larger basis sets. For correlated methods with polynomial scaling, these reductions in the number of orbitals lead to huge savings in computational cost. This behavior is shown in Figure 1(c), where we report the speed-up, calculated as the ratio of time taken for the canonical AFQMC calculation and the total LNO-AFQMC calculation. The time taken for LNO-AFQMC is reported as the sum of times for all fragment calculations, but, because these calculations are independent, the walltime can be reduced by a factor approximately equal to the number of fragments if these calculations are performed in parallel.

In the DZ basis set with a target stochastic error of 1 mHa, the LNO method with the loosest threshold accelerates the

calculations by a factor of about 23; with the tightest threshold, the time becomes comparable to that of canonical AFQMC. Results are even more encouraging in larger basis sets, where the number of orbitals per fragment is a smaller fraction of the total and the speed-up is therefore more significant. In the QZ basis, the speed-up ranges from almost 300 to 3 with an increasingly tight threshold, and even in the latter case, the stochastic error of LNO-AFQMC was converged to 1 mHa while that for canonical AFQMC could only be converged to 2 mHa. Finally, we note that these timings and speed-ups pertain to a relatively small molecule, for which canonical AFQMC calculations are feasible. As shown in the Supporting Information, the speed-up becomes even more pronounced for larger molecules [melatonin (90 valence electrons) and penicillin (128 valence electrons)] where obtaining canonical benchmark results in large basis sets becomes impractical. We conclude that while specific timings are influenced by acceptable errors, molecular size, basis set, and hardware, LNO-AFQMC demonstrates better efficiency compared to its canonical counterpart and scales effectively to larger systems with larger basis sets.

III.II. Isomerization Energies. The relative energy differences between structures during chemical reactions are often more significant than their absolute energies. In order to assess the performance of LNO-AFQMC for chemical reactions, we studied three isomerization reactions from the ISOL database, which contains 24 isomerization reactions of large organic molecules. ^{86,87} As a case study, we focus on reaction 10, shown

in the inset of Figure 2(a). The molecule has 15 heavy atoms, 82 electrons, and 715 orbitals in the cc-pVTZ basis set; it has one of the smallest isomerization energies in the ISOL database, and it is the most challenging of the three reactions that we study. As shown in Figure 2(a), with increasingly tight LNO thresholds, the error in the total energy (with the MP2 correction), for both the reactant and the product, decreases from about 50 to 2-4 mHa. Importantly, the error is very similar for both the reactant and the product at a given threshold such that the energy difference (the isomerization energy) is almost independent of the threshold. In fact, the isomerization energy is always within the relatively large stochastic error bars of the canonical AFQMC calculation, which predicts an isomerization energy of 7 ± 3 kcal/mol. From our tightest threshold, the LNO-AFQMC isomerization energy is predicted to be 6.3 ± 0.9 kcal/mol; for comparison, the LNO-CCSD(T) isomerization energy in the same basis set was calculated as 6.16 kcal/mol. We also note that PT2 correction is necessary for this convergence behavior. Without the correction, similar accuracy is achieved only using the tightest threshold. Additionally, convergence with the threshold is dependent on the nature of the system under consideration. Therefore, it is advisible to perform a convergence test for the studied property using the LNO truncation threshold.

We performed the same calculations for reactions 3 and 9, and detailed results for all reactions are presented in the Supporting Information. In all cases, we find that energy differences converge significantly faster than total energies and are always within the stochastic error of the canonical AFQMC result, even for loose thresholds. In Table 1, we report LNO-

Table 1. Isomerization Energy (kcal/mol) of Reactions 3, 9, and 10 (see the Supporting Information for figures of reactions) Obtained Using LNO-AFQMC, AFQMC, and CCSD(T) in the cc-pVTZ Basis Set^a

	reaction 3	reaction 9	reaction 10
LNO-AFQMC (loosest)	8.8(9)	22.6(9)	8.2(9)
LNO-AFQMC (tightest)	8.8(9)	22.0(9)	6.3(9)
AFQMC	9.4(9)	20(1)	7(3)
CCSD(T)	8.77	21.63	6.16

^aFor reaction 10, because of its large size, we give the result from LNO-CCSD(T) with the tightest threshold.

AFQMC isomerization energies for all three reactions obtained using the loosest and tightest thresholds, compared with canonical AFQMC and CCSD(T) in the cc-pVTZ basis set. The LNO-AFQMC results are in good agreement with those from canonical AFQMC and required only a fraction of the cost. Employing the loosest threshold had a speed-up of 158, 233, and 43 for reactions 3, 9, and 10, respectively (and recall that, for reaction 10, the canonical AFQMC calculation had only reached convergence within a stochastic error of 3 kcal/ mol). As the calculations with looser thresholds are several times faster than that using the tightest, employing such thresholds becomes a practical and computationally viable approach for testing convergence in reaction energy calculations. Even with the tightest threshold, LNO-AFQMC was still faster than the canonical counterpart by a factor of 3 for reactions 3 and 9 and comparable for reaction 10 despite converging to a smaller stochastic error. Moreover, the

agreement with (LNO-)CCSD(T) is quite good, reflecting the single-reference character of these organic molecules.

Interestingly, when using a Trotter time step of 0.005 au, the canonical AFQMC energy calculation for the reactant of reaction 9 showed a notable difference of 7 mHa compared to the LNO-AFQMC calculation. When the time step was halved, this difference reduced to 4 mHa. This behavior can be attributed to the scaling of the Trotter error with system size. However, the LNO-AFQMC approach effectively circumvents these biases by employing fragment calculations that are considerably smaller in scale than the overall system. Similar sensitivity to Trotter time step was observed for the product of reaction 3 in the aug-cc-pVDZ basis set. Notably, the AFQMC calculation with a time step of 0.0025 au closely aligns with the tightest LNO-AFQMC result obtained using a step size of 0.005 au, which demonstrates the reliability of the local method.

IV. CONCLUSIONS

In this work, we introduced local correlation into the AFQMC framework, specifically via the use of local natural orbitals. The LNO framework provides an efficient truncation of the basis set, which makes it possible to perform LNO-AFQMC calculations with basis sets larger than those possible with canonical AFQMC. Notably, energy differences converge much more rapidly than total energies, which makes this method especially promising for applications in chemistry. In the future, LNO-AFQMC will be extended to study open-shell and strongly correlated, multireference systems. To achieve this, we will adapt LNO-AFQMC for use with multideterminantal trial states, 12,88 for which there is no unique set of occupied orbitals and eq 15 no longer holds.

ASSOCIATED CONTENT

Data Availability Statement

PySCF code is available at https://github.com/pyscf/pyscf. AFQMC code can be obtained from Dice at https://github.com/sanshar/Dice. LNO code is under development and can be obtained upon reasonable request from the authors.

Supporting Information

The Supporting Information is available free of charge at https://pubs.acs.org/doi/10.1021/acs.jctc.3c01122.

Details of geometries used, absolute energies, and the average size of the fragments in all calculations (PDF)

AUTHOR INFORMATION

Corresponding Author

Jo S. Kurian — Department of Chemistry, University of Colorado, Boulder, Colorado 80302, United States;
orcid.org/0000-0001-9273-1043; Email: jokurian12@gmail.com

Authors

Hong-Zhou Ye − Department of Chemistry, Columbia University, New York, New York 10027, United States; orcid.org/0000-0002-3714-2753

Ankit Mahajan – Department of Chemistry, University of Colorado, Boulder, Colorado 80302, United States; Department of Chemistry, Columbia University, New York, New York 10027, United States Timothy C. Berkelbach – Department of Chemistry, Columbia University, New York, New York 10027, United States; © orcid.org/0000-0002-7445-2136

Sandeep Sharma — Department of Chemistry, University of Colorado, Boulder, Colorado 80302, United States;
orcid.org/0000-0002-6598-8887

Complete contact information is available at: https://pubs.acs.org/10.1021/acs.jctc.3c01122

Notes

The authors declare no competing financial interest.

ACKNOWLEDGMENTS

This work was supported by the National Science Foundation under Grant Nos. CHE-2145209 (J.S.K.), OAC-1931321, and CHE-1848369 (H.-Z.Y. and T.C.B.), and by a grant from the Camille and Henry Dreyfus Foundation (S.S.). This work utilized resources from the University of Colorado Boulder Research Computing Group, which was supported by the National Science Foundation (Award Nos. ACI-1532235 and ACI-1532236), the University of Colorado Boulder, and Colorado State University.

REFERENCES

- (1) Cohen, A. J.; Mori-Sánchez, P.; Yang, W. Challenges for Density Functional Theory. *Chem. Rev.* **2012**, *112*, 289–320.
- (2) Bartlett, R. J.; Musiał, M. Coupled-cluster theory in quantum chemistry. *Rev. Mod. Phys.* **2007**, *79*, 291–352.
- (3) Motta, M.; Zhang, S. Ab initio computations of molecular systems by the auxiliary-field quantum Monte Carlo method. *WIREs Comput. Mol. Sci.* **2018**, 8, No. e1364.
- (4) LeBlanc, J. P. F.; Antipov, A. E.; Becca, F.; Bulik, I. W.; Chan, G. K.-L.; Chung, C.-M.; Deng, Y.; Ferrero, M.; Henderson, T. M.; Jiménez-Hoyos, C. A.; et al. Solutions of the Two-Dimensional Hubbard Model: Benchmarks and Results from a Wide Range of Numerical Algorithms. *Phys. Rev. X* 2015, 5, No. 041041.
- (5) Motta, M.; Ceperley, D. M.; Chan, G. K.-L.; Gomez, J. A.; Gull, E.; Guo, S.; Jiménez-Hoyos, C. A.; Lan, T. N.; Li, J.; Ma, F.; et al. Towards the Solution of the Many-Electron Problem in Real Materials: Equation of State of the Hydrogen Chain with State-of-the-Art Many-Body Methods. *Phys. Rev. X* 2017, 7, No. 031059.
- (6) Williams, K. T.; Yao, Y.; Li, J.; Chen, L.; Shi, H.; Motta, M.; Niu, C.; Ray, U.; Guo, S.; Anderson, R. J.; et al. Direct Comparison of Many-Body Methods for Realistic Electronic Hamiltonians. *Phys. Rev.* X 2020, 10, No. 011041.
- (7) Rudshteyn, B.; Coskun, D.; Weber, J. L.; Arthur, E. J.; Zhang, S.; Reichman, D. R.; Friesner, R. A.; Shee, J. Predicting Ligand-Dissociation Energies of 3d Coordination Complexes with Auxiliary-Field Quantum Monte Carlo. *J. Chem. Theory Comput.* **2020**, *16*, 3041–3054.
- (8) Eskridge, B.; Krakauer, H.; Zhang, S. Local embedding and effective downfolding in the auxiliary-field quantum Monte Carlo method. *J. Chem. Theory Comput.* **2019**, *15*, 3949–3959.
- (9) Rudshteyn, B.; Weber, J. L.; Coskun, D.; Devlaminck, P. A.; Zhang, S.; Reichman, D. R.; Shee, J.; Friesner, R. A. Calculation of Metallocene Ionization Potentials via Auxiliary Field Quantum Monte Carlo: Toward Benchmark Quantum Chemistry for Transition Metals. J. Chem. Theory Comput. 2022, 18, 2845—2862.
- (10) Lee, J.; Malone, F. D.; Morales, M. A. Utilizing Essential Symmetry Breaking in Auxiliary-Field Quantum Monte Carlo: Application to the Spin Gaps of the C36 Fullerene and an Iron Porphyrin Model Complex. *J. Chem. Theory Comput.* **2020**, *16*, 3019—3027.
- (11) Sukurma, Z.; Schlipf, M.; Humer, M.; Taheridehkordi, A.; Kresse, G. Benchmark Phaseless Auxiliary-Field Quantum Monte

- Carlo Method for Small Molecules. J. Chem. Theory Comput. 2023, 19, 4921–4934.
- (12) Mahajan, A.; Lee, J.; Sharma, S. Selected configuration interaction wave functions in phaseless auxiliary field quantum Monte Carlo. *J. Chem. Phys.* **2022**, *156*, No. 174111.
- (13) Blankenbecler, R.; Scalapino, D. J.; Sugar, R. L. Monte Carlo calculations of coupled boson-fermion systems. I. *Phys. Rev. D* **1981**, 24, 2278–2286.
- (14) Becca, F.; Sorella, S. Quantum Monte Carlo Approaches for Correlated Systems; Cambridge University Press, 2017.
- (15) Al-Saidi, W. A.; Krakauer, H.; Zhang, S. Auxiliary-field quantum Monte Carlo study of TiO and MnO molecules. *Phys. Rev. B* **2006**, 73, No. 075103.
- (16) Malone, F. D.; Zhang, S.; Morales, M. A. Overcoming the Memory Bottleneck in Auxiliary Field Quantum Monte Carlo Simulations with Interpolative Separable Density Fitting. *J. Chem. Theory Comput.* **2019**, *15*, 256–264.
- (17) Motta, M.; Shee, J.; Zhang, S.; Chan, G. K.-L. Efficient Ab Initio Auxiliary-Field Quantum Monte Carlo Calculations in Gaussian Bases via Low-Rank Tensor Decomposition. *J. Chem. Theory Comput.* **2019**, *15*, 3510–3521.
- (18) Weber, J. L.; Vuong, H.; Devlaminck, P. A.; Shee, J.; Lee, J.; Reichman, D. R.; Friesner, R. A. A Localized-Orbital Energy Evaluation for Auxiliary-Field Quantum Monte Carlo. *J. Chem. Theory Comput.* **2022**, *18*, 3447–3459.
- (19) Lee, J.; Reichman, D. R. Stochastic resolution-of-the-identity auxiliary-field quantum Monte Carlo: Scaling reduction without overhead. *J. Chem. Phys.* **2020**, *153*, No. 044131.
- (20) Pham, H. Q.; Ouyang, R.; Lv, D. Scalable Quantum Monte Carlo with Direct-Product Trial Wave Functions. 2023, arXiv:2306.15186. arXiv.org e-Print archive. https://arxiv.org/abs/2306.15186.
- (21) Meyer, W. Ionization energies of water from PNO-CI calculations. *Int. J. Quantum Chem.* **2009**, *5*, 341–348.
- (22) Pulay, P. Localizability of dynamic electron correlation. *Chem. Phys. Lett.* **1983**, *100*, 151–154.
- (23) Pulay, P.; Saebo, S. Orbital-invariant formulation and second-order gradient evaluation in Møller-Plesset perturbation theory. *Theor. Chim. Acta* **1986**, *69*, 357–368.
- (24) Sæbø, S.; Pulay, P. Local configuration interaction: An efficient approach for larger molecules. *Chem. Phys. Lett.* **1985**, *113*, 13–18.
- (25) Sæbø, S.; Pulay, P. Fourth-order Møller-Plessett perturbation theory in the local correlation treatment. I. Method. *J. Chem. Phys.* **1987**, *86*, 914–922.
- (26) Schütz, M.; Hetzer, G.; Werner, H.-J. Low-order scaling local electron correlation methods. I. Linear scaling local MP2. *J. Chem. Phys.* **1999**, *111*, 5691–5705.
- (27) Scuseria, G. E.; Ayala, P. Y. Linear scaling coupled cluster and perturbation theories in the atomic orbital basis. *J. Chem. Phys.* **1999**, 111, 8330–8343.
- (28) Hetzer, G.; Schütz, M.; Stoll, H.; Werner, H.-J. Low-order scaling local correlation methods II: Splitting the Coulomb operator in linear scaling local second-order Møller–Plesset perturbation theory. *J. Chem. Phys.* **2000**, *113*, 9443–9455.
- (29) Schütz, M. Low-order scaling local electron correlation methods. III. Linear scaling local perturbative triples correction (T). *J. Chem. Phys.* **2000**, *113*, 9986–10001.
- (30) Schütz, M. A new, fast, semi-direct implementation of linear scaling local coupled cluster theory. *Phys. Chem. Chem. Phys.* **2002**, *4*, 3941–3947.
- (31) Maslen, P. E.; Dutoi, A. D.; Lee, M. S.; Shao, Y.; Head-Gordon, M. Accurate local approximations to the triples correlation energy: formulation, implementation and tests of 5th-order scaling models. *Mol. Phys.* **2005**, *103*, 425–437.
- (32) Kats, D.; Korona, T.; Schütz, M. Local CC2 electronic excitation energies for large molecules with density fitting. *J. Chem. Phys.* **2006**, 125, No. 104106.
- (33) Kats, D.; Korona, T.; Schütz, M. Transition strengths and first-order properties of excited states from local coupled cluster CC2

- response theory with density fitting. J. Chem. Phys. 2007, 127, No. 064107.
- (34) Edmiston, C.; Krauss, M. Configuration-Interaction Calculation of H3 and H2. J. Chem. Phys. 1965, 42, 1119–1120.
- (35) Ahlrichs, R.; Driessler, F.; Lischka, H.; Staemmler, V.; Kutzelnigg, W. PNO-CI (pair natural orbital configuration interaction) and CEPA-PNO (coupled electron pair approximation with pair natural orbitals) calculations of molecular systems. II. The molecules BeH2, BH, BH3, CH4, CH-3, NH3 (planar and pyramidal), H2O, OH+3, HF and the Ne atom. *J. Chem. Phys.* 1975, 62, 1235–1247.
- (36) Meyer, W. PNO-CI Studies of electron correlation effects. I. Configuration expansion by means of nonorthogonal orbitals, and application to the ground state and ionized states of methane. *J. Chem. Phys.* **1973**, 58, 1017–1035.
- (37) Riplinger, C.; Neese, F. An efficient and near linear scaling pair natural orbital based local coupled cluster method. *J. Chem. Phys.* **2013**, *138*, No. 034106.
- (38) Riplinger, C.; Sandhoefer, B.; Hansen, A.; Neese, F. Natural triple excitations in local coupled cluster calculations with pair natural orbitals. *J. Chem. Phys.* **2013**, *139*, No. 134101.
- (39) Pinski, P.; Riplinger, C.; Valeev, E. F.; Neese, F. Sparse maps—A systematic infrastructure for reduced-scaling electronic structure methods. I. An efficient and simple linear scaling local MP2 method that uses an intermediate basis of pair natural orbitals. *J. Chem. Phys.* **2015**, *143*, No. 034108.
- (40) Riplinger, C.; Pinski, P.; Becker, U.; Valeev, E. F.; Neese, F. Sparse maps—A systematic infrastructure for reduced-scaling electronic structure methods. II. Linear scaling domain based pair natural orbital coupled cluster theory. *J. Chem. Phys.* **2016**, *144*, No. 024109.
- (41) Schwilk, M.; Usvyat, D.; Werner, H.-J. Communication: Improved pair approximations in local coupled-cluster methods. *J. Chem. Phys.* **2015**, *142*, No. 121102.
- (42) Werner, H.-J.; Knizia, G.; Krause, C.; Schwilk, M.; Dornbach, M. Scalable Electron Correlation Methods I.: PNO-LMP2 with Linear Scaling in the Molecular Size and Near-Inverse-Linear Scaling in the Number of Processors. *J. Chem. Theory Comput.* **2015**, *11*, 484–507.
- (43) Ma, Q.; Werner, H.-J. Scalable Electron Correlation Methods. 2. Parallel PNO-LMP2-F12 with Near Linear Scaling in the Molecular Size. *J. Chem. Theory Comput.* **2015**, *11*, 5291–5304.
- (44) Schmitz, G.; Hättig, C. Perturbative triples correction for local pair natural orbital based explicitly correlated CCSD(F12*) using Laplace transformation techniques. *J. Chem. Phys.* **2016**, *145*, No. 234107.
- (45) Hättig, C.; Tew, D. P.; Helmich, B. Local explicitly correlated second- and third-order Møller–Plesset perturbation theory with pair natural orbitals. *J. Chem. Phys.* **2012**, *136*, No. 204105.
- (46) Schmitz, G.; Helmich, B.; Hättig, C. A scaling PNO–MP2 method using a hybrid OSV-PNO approach with an iterative direct generation of OSVs†. *Mol. Phys.* **2013**, *111*, 2463–2476.
- (47) Schmitz, G.; Hättig, C.; Tew, D. P. Explicitly correlated PNO-MP2 and PNO-CCSD and their application to the S66 set and large molecular systems. *Phys. Chem. Chem. Phys.* **2014**, *16*, 22167–22178.
- (48) Yang, J.; Kurashige, Y.; Manby, F. R.; Chan, G. K. L. Tensor factorizations of local second-order Møller–Plesset theory. *J. Chem. Phys.* **2011**, *134*, No. 044123.
- (49) Kurashige, Y.; Yang, J.; Chan, G. K.-L.; Manby, F. R. Optimization of orbital-specific virtuals in local Møller-Plesset perturbation theory. *J. Chem. Phys.* **2012**, *136*, No. 124106.
- (50) Yang, J.; Chan, G. K.-L.; Manby, F. R.; Schütz, M.; Werner, H.-J. The orbital-specific-virtual local coupled cluster singles and doubles method. *J. Chem. Phys.* **2012**, *136*, No. 144105.
- (51) Schütz, M.; Yang, J.; Chan, G. K.-L.; Manby, F. R.; Werner, H.-J. The orbital-specific virtual local triples correction: OSV-L(T). *J. Chem. Phys.* **2013**, 138, No. 054109.
- (52) Williamson, A. J.; Hood, R. Q.; Grossman, J. C. Linear-scaling quantum monte carlo calculations. *Phys. Rev. Lett.* **2001**, 87, No. 246406.

- (53) Manten, S.; Lüchow, A. Linear scaling for the local energy in quantum Monte Carlo. *J. Chem. Phys.* **2003**, *119*, 1307–1312.
- (54) Alfè, D.; Gillan, M. J. Linear-scaling quantum Monte Carlo technique with non-orthogonal localized orbitals. *J. Phys.: Condens. Matter* **2004**, *16*, No. L305.
- (55) Kussmann, J.; Ochsenfeld, C. Linear-scaling fixed-node diffusion quantum Monte Carlo: Accounting for the nodal information in a density matrix-based scheme. *J. Chem. Phys.* **2008**, 128, No. 134104.
- (56) Förner, W.; Ladik, J.; Otto, P.; Čížek, J. Coupled-cluster studies. II. The role of localization in correlation calculations on extended systems. *Chem. Phys.* **1985**, *97*, 251–262.
- (57) Förner, W. Coupled cluster studies. IV. Analysis of the correlated wavefunction in canonical and localized orbital basis for ethylene, carbon monoxide, and carbon dioxide. *Chem. Phys.* **1987**, 114, 21–35.
- (58) Stoll, H. Correlation energy of diamond. *Phys. Rev. B* **1992**, 46, 6700–6704.
- (59) Yu, M.; Kalvoda, S.; Dolg, M. An incremental approach for correlation contributions to the structural and cohesive properties of polymers. Coupled-cluster study of trans-polyacetylene. *Chem. Phys.* **1997**, 224, 121–131.
- (60) Buth, C.; Paulus, B. Basis set convergence in extended systems: infinite hydrogen fluoride and hydrogen chloride chains. *Chem. Phys. Lett.* **2004**, 398, 44–49.
- (61) Willnauer, C.; Birkenheuer, U. Quantum chemical ab initio calculations of correlation effects in complex polymers: Poly(paraphenylene). *J. Chem. Phys.* **2004**, *120*, 11910–11918.
- (62) Rościszewski, K.; Doll, K.; Paulus, B.; Fulde, P.; Stoll, H. Ground-state properties of rutile: Electron-correlation effects. *Phys. Rev. B* **1998**, *57*, 14667–14672.
- (63) Stoll, H. Can incremental expansions cope with high-order coupled-cluster contributions? *Mol. Phys.* **2010**, *108*, 243–248.
- (64) Eriksen, J. J.; Gauss, J. Incremental treatments of the full configuration interaction problem. WIREs Comput. Mol. Sci. 2021, 11, No. e1525.
- (65) Rask, A. E.; Zimmerman, P. M. Toward Full Configuration Interaction for Transition-Metal Complexes. *J. Phys. Chem. A* **2021**, 125, 1598–1609.
- (66) Li, W.; Li, S. Divide-and-conquer local correlation approach to the correlation energy of large molecules. *J. Chem. Phys.* **2004**, *121*, 6649–6657.
- (67) Kobayashi, M.; Nakai, H. Extension of linear-scaling divideand-conquer-based correlation method to coupled cluster theory with singles and doubles excitations. *J. Chem. Phys.* **2008**, *129*, No. 044103.
- (68) Eriksen, J. J.; Baudin, P.; Ettenhuber, P.; Kristensen, K.; Kjærgaard, T.; Jørgensen, P. Linear-Scaling Coupled Cluster with Perturbative Triple Excitations: The Divide–Expand–Consolidate CCSD(T) Model. J. Chem. Theory Comput. 2015, 11, 2984–2993.
- (69) Ziółkowski, M.; Jansík, B.; Kjærgaard, T.; Jørgensen, P. Linear scaling coupled cluster method with correlation energy based error control. *J. Chem. Phys.* **2010**, *133*, No. 014107.
- (70) Kjærgaard, T. The Laplace transformed divide-expand-consolidate resolution of the identity second-order Møller-Plesset perturbation (DEC-LT-RIMP2) theory method. *J. Chem. Phys.* **2017**, *146*, No. 044103.
- (71) Li, S.; Ma, J.; Jiang, Y. Linear scaling local correlation approach for solving the coupled cluster equations of large systems. *J. Comput. Chem.* **2002**, 23, 237–244.
- (72) Li, W.; Piecuch, P.; Gour, J. R.; Li, S. Local correlation calculations using standard and renormalized coupled-cluster approaches. *J. Chem. Phys.* **2009**, *131*, No. 114109.
- (73) Rolik, Z.; Kállay, M. A general-order local coupled-cluster method based on the cluster-in-molecule approach. *J. Chem. Phys.* **2011**. *135*. No. 104111.
- (74) Rolik, Z.; Szegedy, L.; Ladjánszki, I.; Ladóczki, B.; Kállay, M. An efficient linear-scaling CCSD(T) method based on local natural orbitals. *J. Chem. Phys.* **2013**, *139*, No. 094105.

- (75) Nagy, P. R.; Kállay, M. Optimization of the linear-scaling local natural orbital CCSD(T) method: Redundancy-free triples correction using Laplace transform. *J. Chem. Phys.* **2017**, *146*, No. 214106.
- (76) Nagy, P. R.; Samu, G.; Kállay, M. Optimization of the Linear-Scaling Local Natural Orbital CCSD(T) Method: Improved Algorithm and Benchmark Applications. *J. Chem. Theory Comput.* **2018**, *14*, 4193–4215.
- (77) Nagy, P. R.; Kállay, M. Approaching the Basis Set Limit of CCSD(T) Energies for Large Molecules with Local Natural Orbital Coupled-Cluster Methods. *J. Chem. Theory Comput.* **2019**, *15*, 5275–5298.
- (78) Zhang, S.; Krakauer, H. Quantum Monte Carlo method using phase-free random walks with Slater determinants. *Phys. Rev. Lett.* **2003**, *90*, No. 136401.
- (79) Foulkes, W. M. C.; Mitas, L.; Needs, R. J.; Rajagopal, G. Quantum Monte Carlo simulations of solids. *Rev. Mod. Phys.* **2001**, 73, 33–83.
- (80) Sun, Q.; Berkelbach, T. C.; Blunt, N. S.; Booth, G. H.; Guo, S.; Li, Z.; Liu, J.; McClain, J. D.; Sayfutyarova, E. R.; Sharma, S.; Wouters, S.; Chan, G. K.-L. PySCF: the Python-based simulations of chemistry framework. WIREs Comput. Mol. Sci. 2018, 8, No. e1340.
- (81) Sharma, S.; Holmes, A. A.; Jeanmairet, G.; Alavi, A.; Umrigar, C. J. Semistochastic Heat-Bath Configuration Interaction Method: Selected Configuration Interaction with Semistochastic Perturbation Theory. J. Chem. Theory Comput. 2017, 13, 1595–1604.
- (82) Dunning, T. H. Gaussian basis sets for use in correlated molecular calculations. I. The atoms boron through neon and hydrogen. *J. Chem. Phys.* **1989**, *90*, 1007–1023.
- (83) Kendall, R. A.; Dunning, T. H.; Harrison, R. J. Electron affinities of the first-row atoms revisited. Systematic basis sets and wave functions. *J. Chem. Phys.* **1992**, *96*, 6796–6806.
- (84) Woon, D. E.; Dunning, T. H. Gaussian basis sets for use in correlated molecular calculations. III. The atoms aluminum through argon. *J. Chem. Phys.* **1993**, *98*, 1358–1371.
- (85) Pipek, J.; Mezey, P. G. A fast intrinsic localization procedure applicable for ab initio and semiempirical linear combination of atomic orbital wave functions. *J. Chem. Phys.* **1989**, *90*, 4916–4926.
- (86) Huenerbein, R.; Schirmer, B.; Moellmann, J.; Grimme, S. Effects of London dispersion on the isomerization reactions of large organic molecules: a density functional benchmark study. *Phys. Chem. Chem. Phys.* **2010**, *12*, 6940–6948.
- (87) Luo, S.; Zhao, Y.; Truhlar, D. G. Validation of electronic structure methods for isomerization reactions of large organic molecules. *Phys. Chem. Chem. Phys.* **2011**, *13*, 13683–13689.
- (88) Mahajan, A.; Sharma, S. Taming the Sign Problem in Auxiliary-Field Quantum Monte Carlo Using Accurate Wave Functions. *J. Chem. Theory Comput.* **2021**, *17*, 4786–4798.